長崎大学教養部紀要（自然科学篇）第21巻　第1号　1—20（1980年8月）

Quantum Oscillations of Relative Sound Velocity in Bismuth and Tellurium-doped Bismuth*

Masao KOGA

(Received April 25, 1980)

The calculations of the line shapes of the quantum oscillations of the relative sound velocity in bismuth and tellurium-doped bismuth are carried out using Nagai-Fukuyama's theory. The results are compared with experiment and the importance of the vertex correction in calculations of the polarizability functions for bismuth is discussed. Discussion on the line shapes for tellurium-doped bismuth is also given.

§ 1. Introduction

The sound velocity in metals, semimetals and semiconductors changes due to the effect of the magnetic field on the electron-phonon interaction. To obtain the expression of the sound velocity, some workers calculated the dispersion of the sound wave using the electric conductivity, some paid their attention to the thermodynamic relation of the sound velocity and others calculated the phonon self-energy.

Blank and Kaner[1] calculated the phonon self-energy in the presence of the magnetic field and obtained the relative sound velocity and the attenuation coefficient from the real and imaginary parts of the phonon self-energy, respectively. There, however, the space charge field resulting from the passage of the sound waves was not taken into account explicitly and was considered to reduce the electron-phonon coupling constant.

In our previous work[2], the phonon self-energy was shown to be expressed with the electron polarizability functions and the electron-phonon coupling constants. The screening effect was explicitly taken into account. The qualitative agreement in the renormalization of the sound velocity in bismuth was obtained in the relaxation time approximation. On the other hand, Nagai and Fukuyama[3] showed in the calculation of the attenuation coefficients in bismuth that the self-consistent Born approximation and the vertex correction are really important for the calculation of the phonon self-energy in the presence of the impurity scattering.

In this work, using Nagai-Fukuyama's theory, we shall give calculations of the relative sound velocity and discuss the results comparing with our experimental data for bismuth and tellurium-doped bismuth.

---

* This work is based on the thesis submitted in partial fulfillment of the requirements for the degree of Doctor of Science at Kyushu University(1978).

§ 2. Theory of the renormalization of the velocity of sound in a semimetal

In the quantum theory, the sound waves are treated as phonons with long wavelengths. In the second quantized form, the carrier–phonon coupling Hamiltonian is given by

$$H_{el-ph} = \frac{1}{V}\sum_{qk\alpha} g_q^{\alpha}(b_q - b_{-q}^{+})c_{k+q}^{\alpha+}c_k^{\alpha}, \qquad (2-1)$$

where V is the volume of the crystal, $b_q(b_q^{+})$ and $c_k^{\alpha}(c_k^{\alpha+})$ are the annihilation (the creation) operators of the phonons with a wave vector q and those of the α–th carriers with a wave vector k, respectively. The coupling constant g_q^{α} is given by

$$g_q^{\alpha} = \sum_{i,j} i(\hbar/8\rho\omega_q)^{1/2}\ (\varepsilon_i q_j + \varepsilon_j q_i)\Lambda_{ij}^{\alpha}, \qquad (2-2)$$

where ρ is the density of the crystal, ε is the polarization vector of the phonon and Λ_{ij}^{α} is the deformation potential tensor for the α–th carriers. The deformation potential tensors for bismuth were theoretically calculated by Katsuki[4] by means of the pseudopotential method.

The renormalized phonon frequency at a finite temperature is derived from the thermodynamic phonon self–energy which can be calculated by using Feynman diagram techniques. Theoretical calculations have been made by Blank and Kaner in the absence of the impurity scattering and by Liu and Toxen[5], and Nagai and Fukuyama in the presence of the impurity scattering. Their results have been obtained under the condition of the strong magnetic field and are applicable only to the single carrier case (for example, a metal). When several groups of carriers are present, the Coulomb interaction between carriers gives serious effects on the renormalization process. Such investigations have been carried out by Kobayashi and Yamada[6] by the method of the quantum–equation–of–motion in the absence of the impurity scattering. As will be shown later, the impurity scattering is important in the quantum oscillations of the sound velocity in a strong magnetic field. Therefore, we have extended Nagai–Fukuyama's theory to the multi–carrier case. In this section we will consider the system with two types of isotropic carriers(electrons and holes) for simplicity.

According to Nagai and Fukuyama, the relative sound velocity and the attenuation coefficient are given, respectively, by

$$\Delta V/V_0 = (1/\hbar\omega_q)\mathrm{Re}[\Pi_{ph}(q,i\omega_\lambda)]_{i\omega_\lambda\to\omega_q+i0}, \qquad (2-3a)$$

$$\alpha = -(2/\hbar V_0)\mathrm{Im}[\Pi_{ph}(q,i\omega_\lambda)]_{i\omega_\lambda\to\omega_q+i0}, \qquad (2-3b)$$

where $\Pi_{ph}(q,i\omega_\lambda)$ is the thermodynamic phonon self–energy and V_0 is the unrenormalized sound velocity.

The phonon self–energy Π_{ph} is a sum of the self–energies due to the interaction with electrons and holes as diagramatically shown in Fig. 1a.

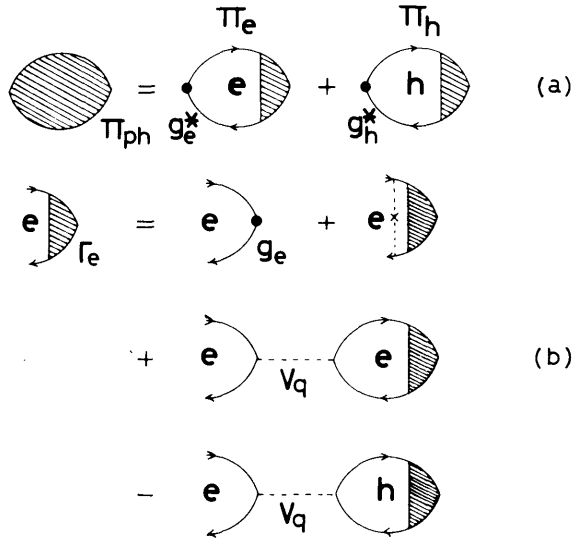

Fig. 1. (a) Diagram for the self-energy of phonons in the system of electrons and holes. (b) Vertex part of the polarizability for electrons.

$$\Pi_{ph} = g_e^* \pi_e + g_h^* \pi_h \ . \qquad (2-4)$$

The vertex parts Γ_e and Γ_h contain all the interactions, such as electron(hole)-phonon, electron-electron(hole-hole), electron-hole and electron(hole)-impurity interactions, as shown in Fig. 1b for Γ_e. From this and the similar one for Γ_h, we obtain the followin equations for π_e and π_h.

$$\pi_e = g_e P_e - V_q(\pi_e - \pi_h)P_e \ , \qquad (2-5a)$$

$$\pi_h = g_h P_h - V_q(\pi_h - \pi_e)P_h \ , \qquad (2-5b)$$

where P_e and P_h are the thermodynamic polarizability function of electrons and that of holes, respectively, and $V_q(=4\pi e^2/\varepsilon_0 q^2)$ is the Coulomb potential. In deriving eqs. (2-5a) and (2-5b), we made an assumption that the impurity potential is of the form of the Dirac delta function. Nagai and Fukuyama did not take account of the Coulomb interaction. In that case, the phonon self-energy is given by

$$\Pi_{ph}(q,i\omega_\lambda) = |g_e|^2 P_e(q,i\omega_\lambda) + |g_h|^2 P_h(q,i\omega_\lambda) \ , \qquad (2-6)$$

Expressing π_e and π_h with P_e and P_h, and substituting them into eq. (2-4), we obtain the expression for the phonon self-energy π_{ph}.

$$\Pi_{ph} = [1 + V_q(P_e + P_h)]^{-1}[|g_e|^2 P_e + |g_h|^2 P_h + V_q|g_e + g_h|^2 P_e P_h] \qquad (2-7)$$

Using eqs. (2-3a) and (2-3b), we obtain the expressions for the relative sound velocity and the attenuation coefficient.

$$\Delta V/V_0 = (-1/2\rho V_0^2)\,|\Lambda_e + \Lambda_h|^2 \mathrm{Re}[P_e P_h/(P_e + P_h)]\,, \qquad (2-8a)$$

$$\alpha = (q/\rho V_0^2)\,|\Lambda_e + \Lambda_h|^2 \mathrm{Im}[P_e P_h/(P_e + P_h)]\,, \qquad (2-8b)$$

where we used the inequality $V_q P_{e,h} \gg 1$ which is in general satisfied in the frequency region of sound wave.

According to Nagai and Fukuyama, when q is small and parallel to the magnetic field, the vertex corrected polarizability function of the carrier in a strong magnetic field is given by

$$P(q,\omega_q) = (iN_o/V)\int d\varepsilon\Big[\nu_q \frac{Q(\varepsilon)}{1 - 2cu^2 Q(\varepsilon)} + \frac{1}{2}\sum_n \partial z_n/\partial\varepsilon - i\sum_n \rho_n(\varepsilon - \nu_q)\Big]\frac{1}{4}\cosh^{-2}[(\varepsilon + \varepsilon_n)/2]\,, \qquad (2-9)$$

where $Q(\varepsilon)=\sum_n \rho_n/(D_n \varepsilon_q + \tau - i\nu_q)$. In the above equation, the level broadening of the energy level is taken into account through the self-consistent Born approximation and the meanings of the various symbols are the same as in ref. (3).

§ 3. Experimental Procedure

The single crystal of bismuth was grown from a melt of zone-refined ingots by the Czochralski vertical pulling technique in an argon atmosphere using a seed crystal. The direction of the crystallographic axes were determined by the Laue X-ray back reflection method. The single crystal ingot was cut into a rectangular parallelpiped by a Servomet cutting machine. The faces of the sample were planed as flat and parallel as possible by the spark planer. Before being used for measurements, the sample was annealed at a constant temperature of about 200 °C for more than 120 hours.

The single crystal of tellurium-doped bismuth was obtained by the horizontal zone levelling technique. The tellurium concentration is above the value where the hole carriers disappear.

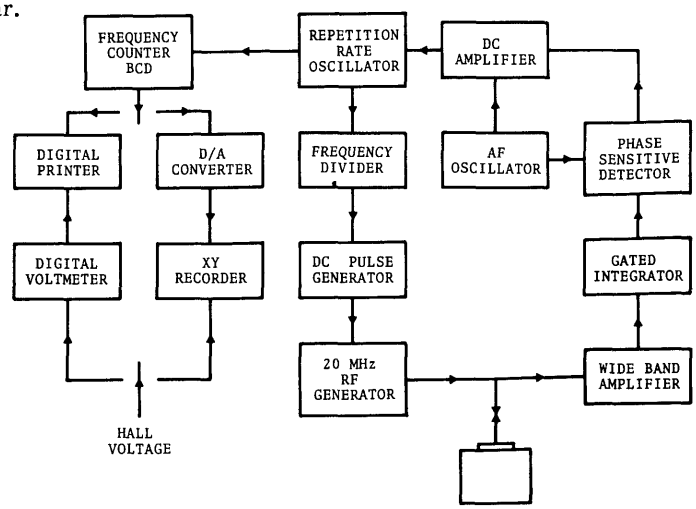

Fig. 2. Blockdiagram of the system for the sound velocity measurement.

The measurements of small changes of the sound velocity were carried out using conventional pulse-echo superposition technique. Longitudinal ultrasonic waves of 20 MHz were excited by an X-cut quartz transducer with a fundamental frequency of 20 MHz. Bonding was with a silicon grease and was repeated until a good echo pattern was obtained. A blockdiagram of the arrangement is shown in Fig. 2. The sensitivity to small changes was generally 1×10^{-6}. In this method, further smaller changes of the sound velocity could be detected using the longer gate time of the universal counter.

In order to attain the low temperature, we evacuated the evaporating gas of liquid helium with an oil rotary pump (4.2 K>T>1.7 K) and with a Kenny pump (1.7 K>T>1.15 K).

Static magnetic fields up to 23 kOe were provided by an electromagnet with the pole piece gap of 65 mm. The current stability is about 10^{-4}. The magnetic field intensity was measured by the Hall probe calibrated against NMR. We could obtain a strictly linear relationship between the field intensity and the Hall voltage in the range from 1.5 kOe to 23 kOe.

§ 4. Expermental Results

The relative sound velocity $\Delta V/V_0$ can be expressed as

$$\Delta V/V_0 = -(1/2\rho V_k^2)\mathrm{Re}[\sum_{i>j} G_{ij}^k P_i P_j / \Sigma P_i] , \qquad (4-1)$$

where k denotes the propagation direction of the logitudinal sound waves and i and j denote the types of the carriers. The values of G_{ij}^k are calculated using the bare deformation potential constants obtained by Katsuki and the elastic constants by Eckstein et al.[7] and are listed in Table I.

Table I. Values of G_{ij}^k calculated using the bare deformation potential constants obtained by Katsuki and the elastic constants by Eckstein et al.

	$G_{ab} = G_{ac}$	G_{ah}	$G_{bh} = G_{ch}$
q//x	24.9	0.33	6.20
q//y	22.0	34.3	1.35
q//z	0.0	39.8	39.8

in units of eV^2.

The Fermi surface of bismuth consists of three electron ellipsoids tilted in the mirror planes at the L-points and one prolate hole ellipsoid at the T-point in the first Brillouin zone. The three equivalent right-handed systems are shosen as such in the Fig. 3a. We give each of the electron ellipsoids a name for convenience. The schematic energy level diagram is also shown in Fig. 3b.

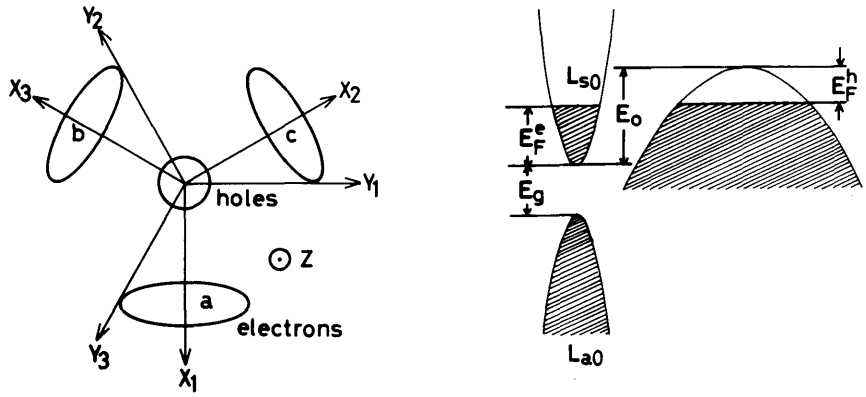

Fig. 3. (a) Schematic diagram of the Fermi surface of bismuth. (b) Schematic energy level diagrams of electrons and holes.

As shown in the previous work, the quantum oscillations of the relative sound velocity due to the b– and c–electrons are absent for $q//y$ and dominant for $q//x$. These were explained by the renormalization and the anisotropy of the deformation potential tensor. We will show and discuss the experimental results for $q//y$ in the following, in connection with the line shape of the quantum oscillations of the relative sound velocity.

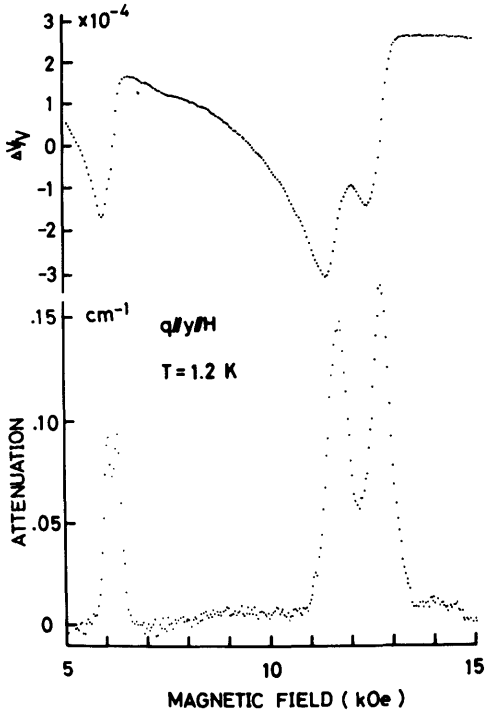

Fig. 4. Quantum oscillations of the sound velocity (a) and the attenuation coefficient. (b) for $q//y//H$ at T = 1.2 K in bismuth.

In Fig. 4, the quantum oscillations of the sound velocity and the attenuation coefficient for $q//y//H$ are plotted using the data recorded with a digital printer.

The characteristics of the results are summarized as follows:

1. The line shape of the attenuation is spike-like and the spin splittings are clear even for the 20 MHz sound waves.

2. The peak at a higher field of the spin-split peaks is larger than the one at a lower field.

3. The attenuation coeffcient has peaks at higher fields than the velocity oscil - lations. The magnetic field of the attenuation peak and that of the velocity minimum do not coincide. The differences between the magnetic fields of the peaks in the attenuation coefficients and those of the corresponding minima of the relative sound velocity are listed in Table II.

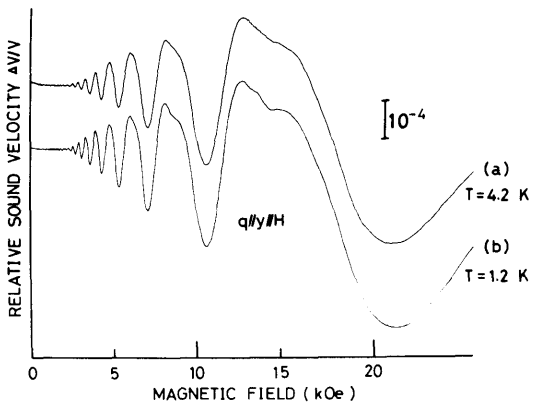

Fig. 5. Quantum oscillations of the sound velocity in tellurium-doped bismuth for $q//y//H$.
(a) T = 4.2 K ; (b) T = 1.2 K.

In Fig. 5, the quantum oscillations of the sound velocity in tellurium-doped bismuth are shown for $q//y//H$ at two different temperatures of T=4.2 K and T=1.2 K. The Fermi energy was increased by the tellurium doping, because tellurium acts as a donor in bismuth. The minima of the sound velocity shift to higher magnetic fields. The period of the velocity oscillations due to the a-electrons, which is proportional to the inverse of the cross-section of the Fermi surface, has been changed from 8.3×10^{-5} Oe^{-1} to 4.9×10^{-5} Oe^{-1}.

The line shape of the oscillations became broader and more symmetric because the Landau levels are broadened due to the tellurium doping. The line shapes less depend on temperature. The amplitude of the oscillations at high fields is still large and amounts to 7×10^{-4} larger than 5.5×10^{-4} in pure bismuth, even though the collision time should be very short as compared with that of pure bismuth. The fact that the amplitude of the oscillations of the sound velocity was not much affected by the impurity scattering suggests the usefulness of the measurement of the sound velocity oscillations in studying the electronic structures of compounds and alloys where the impurity scatterings are very large.

§ 5. Discussion

In this section, we will discuss the observed quantum oscillations of the sound velocity as quantitatively as possible. In calculating the polarizability function, we used band parameters[8], bare deformation potential constants[4], and elastic constants[7] given in the literatures.

a. Bismuth

The electronic energy state of carriers in bismuth depends on the spin quantum number s as well as on the orbital quantum number n. If we assume that the spin-flip transition does not occur in the course of the impurity scattering, the important part of the polarizability function given by Nagai and Fukuyama can be rewritten in the following form.

$$P(q,\omega) = (N_0/V)\sum_s \int_{-\infty}^{\infty} d\varepsilon \Phi^s(\varepsilon) \frac{1}{4}\cosh^{-2}[(\varepsilon + \varepsilon_{ns})/2] , \qquad (5-1)$$

where the energy ε is measured from the Fermi level and is normalized by k_BT. The quantity ε_{ns} represents the bottom of the Landau level with the quantum number (n, s). We defined the line shape function $\Phi^s(\varepsilon)=\Phi_r^s(\varepsilon)+i\Phi_i^s(\varepsilon)$ by

$$\Phi^s(\varepsilon) = \sum_n [\rho_{ns}(\varepsilon) + i\nu_q Q_{ns}(\varepsilon)/\{1 - 2cu^2 Q_s(\varepsilon)\}] . \qquad (5-2)$$

The factor $1/\{1 - 2cu^2 Q_s(\varepsilon)\}$ is the vertex correction due to the impurity scattering and $Q_s(\varepsilon)$ is defined by

$$Q_s(\varepsilon) = \sum_n Q_{ns}(\varepsilon) = \sum_n \rho_{ns}(\varepsilon)/[D_{ns}(\varepsilon)\varepsilon_q + \tau_s - i\nu_q] , \qquad (5-3)$$

where $\varepsilon_q=\hbar^2q^2/2m_z\ k_BT$ and $\nu_q=\hbar\omega_q/k_BT$. The collision rate τ_s is related to the density of states ρ_s by

$$\tau_s = 2cu^2 \rho_s(\varepsilon) = 2cu^2 \sum_n \rho_{ns}(\varepsilon) . \qquad (5-4)$$

Equation (5-4) means that, for the short range impurity potential, the collision rate is a function of energy and is independent of the quantum number n. This may be due to the fact that the short range potential allows for all the inter-Landau level transitions with equal probabilities, so that the collision rate does not depend on the initial state of the carriers.

The normalized density of states $\rho_s(\varepsilon)=\sum_n \rho_{ns}(\varepsilon)$ is related to the imaginary part of the z_s-function defined by

$$z_s = \sum_n z_{ns} = -\sum_n [-(\varepsilon - \varepsilon_{ns}) + cu + cu^2 z_s]^{-1/2} . \qquad (5-5)$$

The diffusion constant D_{ns} in eq. (5–3) is defined by

$$D_{ns}(\varepsilon) = \text{Im } z_{ns}/\text{Re } z_{ns} . \qquad (5-6)$$

When the magnetic field is so strong that the separation between the successive Landau levels is wide enough to neglect the overlap of the density of states due to the different Landau levels, we can drop the summation over n and s. This is the case that Nagai and Fukuyama have applied their theory to the quantitative analysis of the line shape of the giant quantum oscillations of the attenuation coefficient in bismuth and may be called as the single level approximation (SLA). By this approximation, we can see how the vertex correction works in the quantum oscillation of the polarizability function. The line shape function is now simply given by (dropping the spin quantum number s)

$$\Phi(\varepsilon) = [D^2 + iRD]/[D^2 + R^2] , \qquad (5-7)$$

where $R = \nu_q / \varepsilon_q$. The energy dependence of Φ is largely determined by the diffusion constant D which is monotonically increasing funciton of ε. The positions of the maxima of the line shape functions depend on the value of R which is estimated to be 10^3 for the 20 MHz sound wave. In Fig. 6, we show the density of states and the line shape

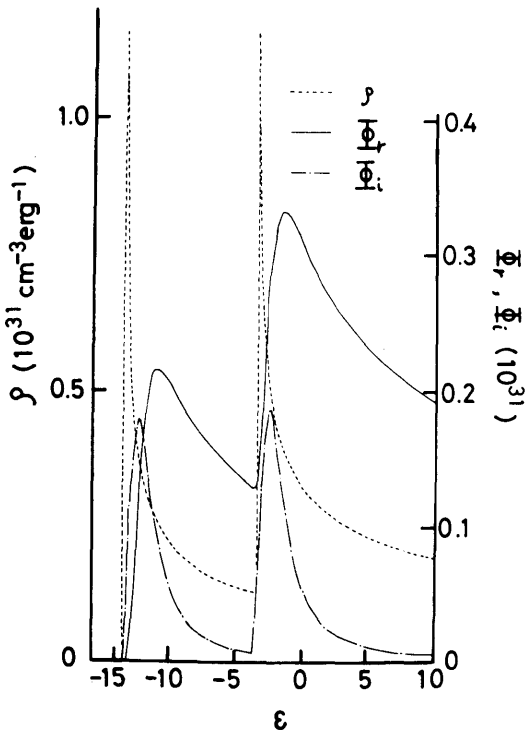

Fig. 6. Calculations of the density of states and the line shape function of the a-electrons in bismuth as a function of energy ε for $q//y//H$, H = 11.5 kOe and T = 1.2 K.

function as a function of energy. It can be seen that the maximum of $\Phi_r(\varepsilon)$ occurs always at higher energy than that of $\Phi_i(\varepsilon)$ which explains the shift of the position of the minima of the sound velocity with respect to the attenuation peak as observed in

the experiments.

It should be noted that without the vertex correction the real part of the polarizability function is almost completely determined by the density of states because $\tau_s >> \nu_q$

In the SLA, the vertex correction becomes very large because the complete cancellation takes place in the denominator

$$\tau = 2\mathrm{cu}^2 \rho . \qquad (5-8)$$

However, the density of states of the particular Landau level has a long tail on the higher energy side, so that the transition to the levels with lower quantum number, even if its density of states is very small, breaks the condition of the complete cancellation and may affect the line shape function. For this reason, we calculated the polarizability function in the approximation in which the summation over n in eqs. (5–1) through (5–5) are taken over all the levels below the Fermi level ($\varepsilon_{ns} \geqq 0$). We shall call this approximation the multi-level approximation (MLA).

In calculating z_s according to eq. (5–5) (self-consistent Born approximation), we neglected cu and the real part of z_s in the right hand side of the equation. This neglect is usually made in the impurity scattering problems. Then, τ_s and D_{ns} are simply given, respectively, by

$$\tau_s = 2\mathrm{cu}^2 \sum_n [\varepsilon - \varepsilon_{ns} + \{(\varepsilon - \varepsilon_{ns})^2 + \tau_s^2/4\}^{1/2}]/2[(\varepsilon - \varepsilon_{ns})^2 + \tau_s^2/4] , \qquad (5-9a)$$

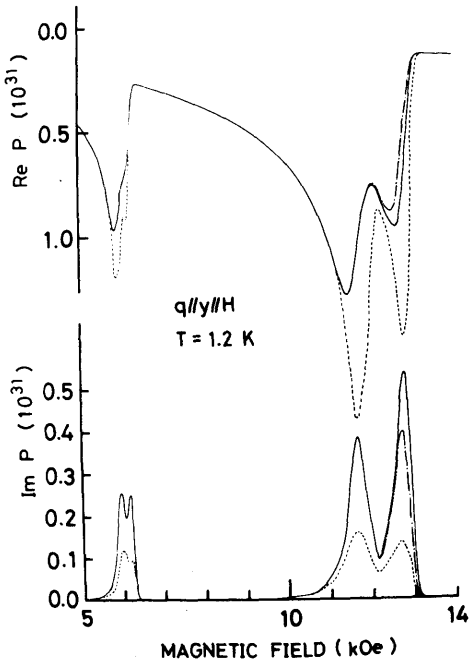

Fig. 7. Polarizability functions for the a-electrons in bismuth for $q//y//H$ at T = 1.2 K. The solid lines are calculated with the vertex correction and the dotted ones without it by the MLA. The dash-dot ones are obtained by the SLA.

$$D_{ns} = (2/r_s)[\varepsilon - \varepsilon_{ns} + \{(\varepsilon - \varepsilon_{ns})^2 + r_s^2/4\}^{1/2}] . \qquad (5-9b)$$

First, we calculated r_s from eq. (5-9a) self-consistently. Then the line shape function was calculated for the given value of ε. The polarizability function was obtained by integrating the line shape function numerically.

In Fig. 7, the calculated polarizability functions of the a-electrons are shown for $q//y//H$. The solid curves, the dotted ones and the dash-dot ones correspond, respectively, to thoes calculated by the MLA with the vertex correction, the MLA without vertex correction and the SLA. The vertex correction affects the line shape and the absolute value of both the real and imaginary parts, especially near the extrema. The peak of the imaginary part is seriously enhanced, while the peak in the real part is reduced by the vertex correction. The difference between the MLA and SLA consists most significantly in the relative height of the two split-off peaks in the imaginary part. The peak at the lower field is due to the (0,+1) level, so that there is no inter-Landau level transition, while the peak due to the (1,−1) level suffers the inter-Landau level transition to the (0,−1) level. Therefore, the (1,−1) peak may be more enhanced in the MLA than in the SLA by the vertex correction.

If the vertex correction is not taken into account, the peaks in the imaginary part of p is rather density of states-like in contradiction with experiment and the (0,+1) peak is higher than the (1,−1) peak. Thus, the vertex correction is important at a strong magnetic field near the quantum limit. In the following, we shall show the calculations of the polarizability functions by the MLA. In Fig. 8, and Fig. 9 are shown the calcu-

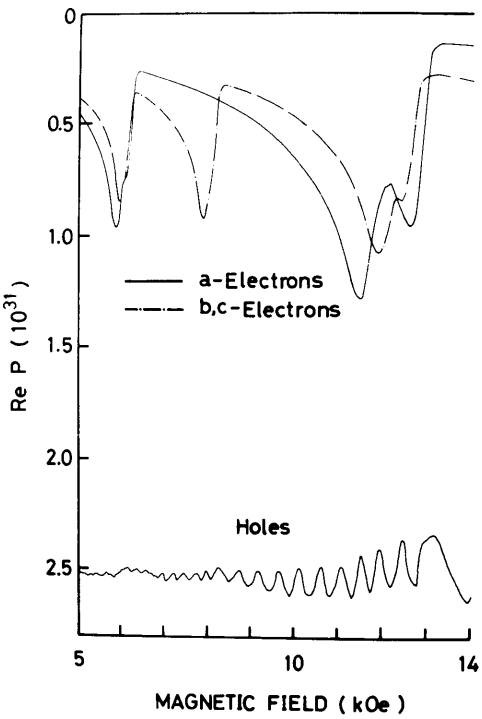

Fig. 8. Real parts of the polarizability functions of the electrons and holes in bismuth for $q//y//H$ at T = 1.2 K.

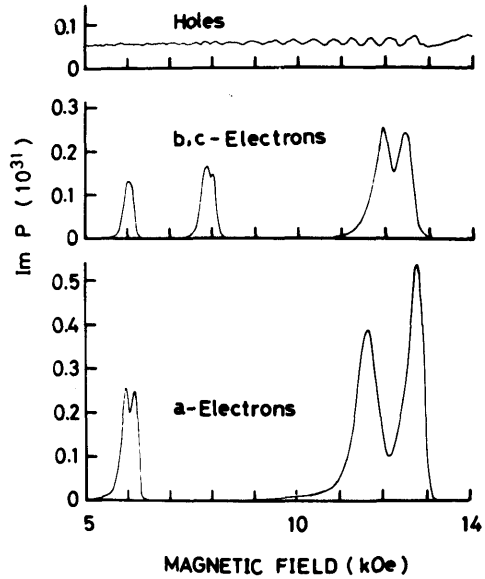

Fig. 9. Imaginary parts of the polarizability functions of the electrons and holes in bismuth for $q//y//H$ at T = 1.2 K.

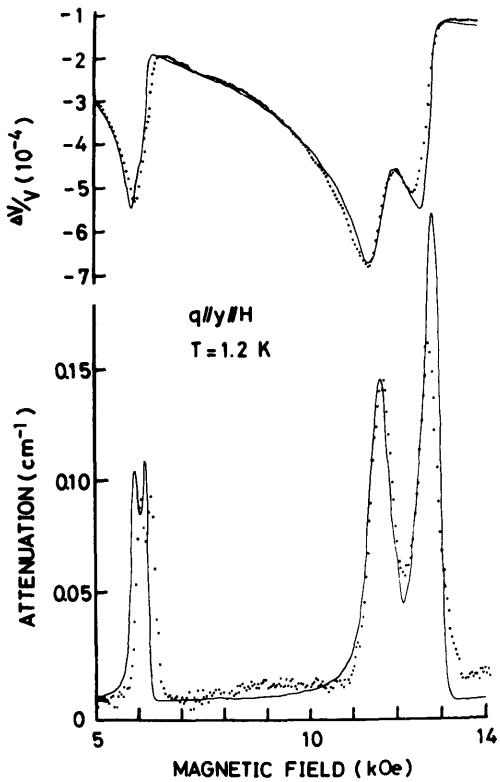

Fig. 10. Calculated curves of the quantum oscillations of the sound velocity and the attenuation coefficient in bismuth for $q//y//H$ at T = 1.2 K together with the experimental curves. The bare deformation potential constants by Katsuki and the elastic constants by Eckstein et al. were used.

lated real and imaginary parts of the polarizability functions of electrons and holes for $q//y//H$. It is seen that the polarizability function of holes are modulated by the magnetic field dependence of the Fermi energy.

By using these results, we calculated the relative sound velocity and the attenuation coefficient according to the relations

$$\Delta V/V_0)_y = -(1/2\rho V_y^2)\mathrm{Re}[\sum_{i>j} G^y_{ij} P_i P_j / \sum_i P_i] , \qquad (5-10a)$$

$$\alpha = (q/\rho V_y^2)\mathrm{Im}[\sum_{i>j} G^y_{ij} P_i P_j / \sum_i P_i] . \qquad (5-10b)$$

The numerical values of G^y_{ij} are listed in Table I. In Fig. 10, the calculated results are shown together with the experimental data. It can be seen that the relative sound velocity is well reproduced by the theoretical calculation. The slight discrepancies may be due to the inadequate choices of the pand parameters. It should be noted, however, that we could not fit the last (1,−1) peak to the theoretical curve by changing the parameter $2cu^2$. The agreement between theory and experiment in the attenuation coefficient is not so satisfactory. The difference of the amplitudes of the spin-split peaks is too large, though the main features could be reproduced, especially, the line shapes are spike-like even at 20 MHz, which proves the importance of the vertex correction. Another evidence of the necessity of the vertex correction is the shifts of the positions of the attenuation peaks relative to the positions of the minima of the sound velocity. The reason is clear in Fig. 6. The numerical values of the shifts are compared with experimental values in Table II.

(n , s)	ΔH	
	Experiment	Theory
(1 ,-1)	325 Oe	150 Oe
(0 ,+1)	300 Oe	250 Oe

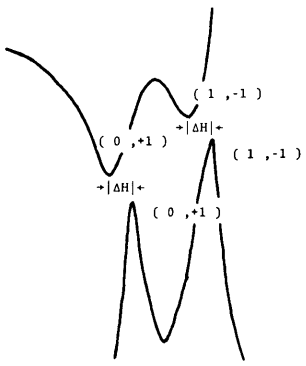

Table II. Differences between the peak positions of the attenuation coefficient and the corresponding minima of the relative sound velocity.

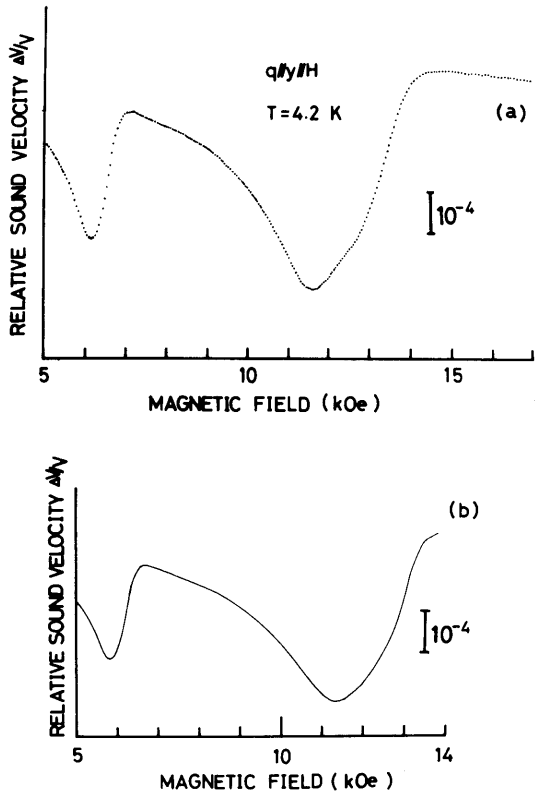

Fig. 11. Calculated sound velocity oscillations in bismuth for $q//y//H$ at T = 1.2 K. (b) together with the experimental result (a).

Figure 11 shows the experimental (a) and the theoretical (b) velocity changes at 4. 2 K for $q//y//H$. The agreement between theory and experiment seems good except for the fact that the absolute amplitude of the oscillation of the theoretical curve is slightly smaller than that of the experimental curve.

From the above considerations, we conclude that the quantum oscillations of the velocity of sound in pure bismuth are quantitatively explainable by Nagai–Fukuyama's theory. The vertex correction to the polarizability function is found to be important.

It should be noted, however, that the above calculations were made with the value of $2cu^2$ which is 0.1 times as large as the one used by Nagai and Fukuyama. With larger values of $2cu^2$, the line shapes become unrealistic irrespective of the SLA or MLA. The above value corresponds to the zero magnetic field scattering time $\tau = 6 \times 10^{-9}$ sec which is too long as compared with the experimental value[9]. Because R in eq. (5–7) is very large at 20 MHz, we must use such an unrealistic scattering time to get the quanti – tative agreement between theory and experiment. The vertex correction in Nagai–Fukuyama's theory, though it is important, seems to become overcorrection at low frequencies.

b. Tellurium–doped bismuth

The same method is applied to calculate the line shapes of the relative sound velocity oscillations for the tellurium–doped sample. The impurity concentration in the doped sample may be two or three orders of magnitude higher than that in bismuth.

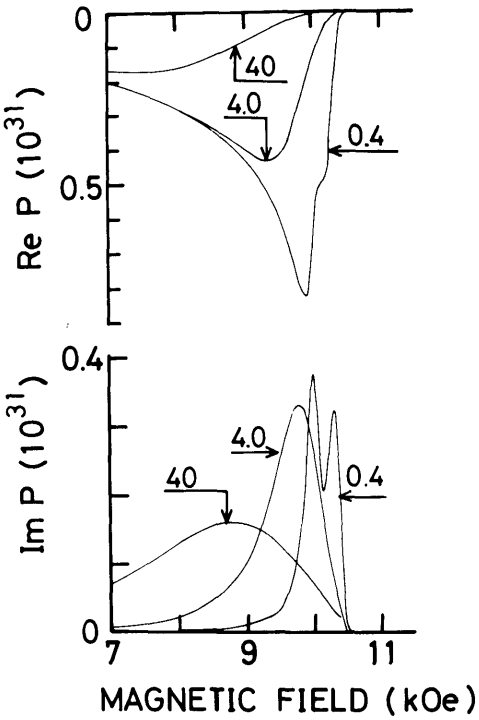

Fig. 12. Calculations of the polarizability functions of the a-electrons in tellurium-doped bismuth by the SLA for $2cu^2$ as a parameter for $q//y//H$ at T = 1.2 K.

Figure 12 shows the polarizability functions of the a-electrons calculated by the SLA with $2cu^2$, normalized with the value used by Nagai and Fukuyama for bismuth, as a parameter for $q//y//H$. As can be seen there, the real part of the polarizability function rapidly decreases with increasing impurity concentration. When $2cu^2$ is about 400 times as large as that in bismuth, the peak in Re P_a almost disappears. Contrary to the theoretical calculations, we observed rather enhanced amplitude in the doped sample, though the line shapes are rather broad. The reason for the reduction of the amplitude in the theoretical calculations can be understood from the SLA line shape function, eq. 5-7 combined with eqs. 5-9a and 5-9b. The collision rate τ becomes large with increasing impurity concentration, so that the energy dependence of D becomes weak. Because R is very large ($\sim 10^3$) at 20 MHz, the maxima of the line shape function are located at energy far apart from $\varepsilon = \varepsilon_{ns}$, where the density of states is considerably small. Thus, we considered that the vertex correction is, by some unknown reasons, ineffective in the doped sample. This may be partly due to the long range nature of the impurity potential of the screened Coulomb type with the screening length of about 40 Å. By this assumption, we can approximate the real part of the line shape function by the density of states and obtain

$$\text{Re } P(q,\omega) = (N_0/V)\sum_{ns} \int_{-\infty}^{\infty} d\varepsilon \, \rho_{ns}(\varepsilon) \frac{1}{4} \cosh^{-2}[(\varepsilon + \varepsilon_{ns})/2] \, . \qquad (5-11)$$

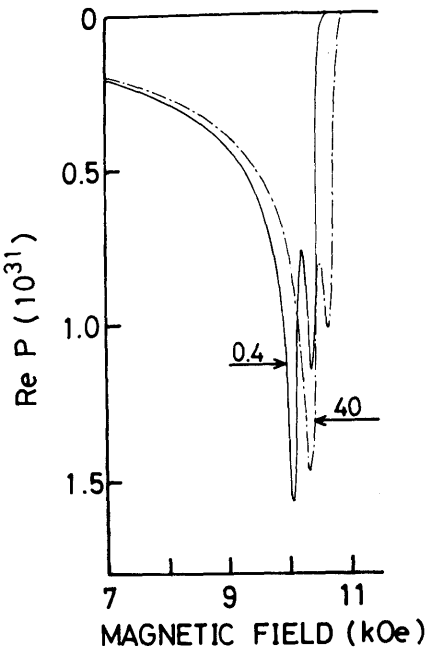

Fig. 13. Calculations of the polarizability functions according to eq. 5–11.

In Fig. 13, we show the real part of the polarizability function calculated according to the above expression. It is seen that the density of states itself does not so much depend on the parameter $2cu^2$. The observed enhancement of the amplitude of the oscillation may be due to the cancellation of the reduction of the peak in the density of states by the increase of the Fermi energy. In order to get the more realistic line shape, it is also necessary to take account of all the higher order terms in Fig. 14 in calculating the density of states of electrons.

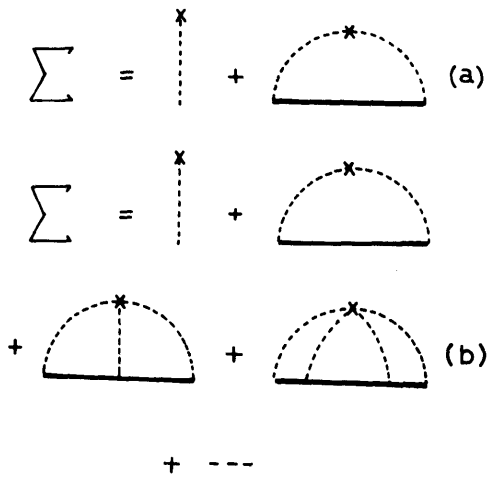

Fig. 14. (a) Self-energy function of electrons in the self-consistent Born approximation.
(b) T-matrix approximation.

§ 6. Conclusion

The line shapes and amplitudes of the velocity oscillations in bismuth could be well reproduced by the calculation of the real part of the phonon self-energy using Nagai-Fukuyama's theory. The vertex correction to the polarizability function is found to be important expecially at strong magnetic fields near the quantum limit.

In the case of a tellurium-doped sample, however, the line shapes and amplitudes of the velocity oscillations could not be reproduced. Despite of the short collision time due to the tellurium doping, the amplitude of the oscillation is still large. The line shapes are rather symmetric. The vertex correction seems to be unnecessary in the doped sample by unknown reasons. Thus, the quantum oscillations of the sound velocity may be solely determined by the density of states. The density of states should be calculated by the T-matrix approximation where the infinite series of the scattering terms are summed.

Acknowledgements

The author should like to express his hearty thanks to Professor Shuzo Takano of Kyushu University for valuable suggestions and stimulating discussions throughout the work.

References

1) A. Ya. Blank and E. A. Kaner : Zh. eksper. teor. Fiz. **50** (1966) 1013.
2) M. Koga and S. Takano : J. Phys. Soc. Japan **42** (1977) 853.
3) T. Nagai and H. Fukuyama : J. Phys. Soc. Japan **41** (1976) 1137.
4) S. Katsuki : J. Phys. Soc. Japan **26** (1969) 696.
5) S. H. Liu and A. M. Toxen : Phys. Rev. **138** (1965) A487.
6) M. Kobayashi and K. Yamada : J. Phys. Soc. Japan **31** (1971) 1306 ; **34** (1973) 959.
7) Y. Eckstein, A. W. Lawson and D. H. Reneker : J. Appl. Phys. **31** (1960) 1534.
8) G. E. Smith, G. A. Baraff and J. M. Rowell : Phys. Rev. **135** (1964) A1118.
9) A. L. Zitter : Phys. Rev. **127** (1962) 1471.

Appendix

The semiclassical equation-of-motion method can easily take account of the Coulomb interaction between carriers, the anisotropy of the deformation potential tensor as well as that of the elastic properties of the crystal(*). The expression for the relative sound velocity is obtained using the longitudinal conductivity. Then using the relation $ie^2\omega P(q,\omega) = q^2\sigma(q,\omega)$ the expression is obtained in terms of the polarizability functions.

For $q//y//H$, the relative sound velocity of the quasi-longitudinal mode is expressed as

$$\Delta V/V_0)_y = -(1/2\rho V_y^2)\,\mathrm{Re}\Big[\sum_{i>j} G^y_{ij} P_i P_j / \sum_i P_i\Big] ,$$

where G^y_{ij} are defined by

$$G^y_{ab} = \alpha\frac{9}{16}(\Lambda^e_1 - \Lambda^e_2)^2 + \beta\frac{9}{4}\Lambda^{e2}_4 + \gamma\frac{6}{8}\Lambda^e_4(\Lambda^e_1 - \Lambda^e_2) ,$$

$$G^y_{ah} = \alpha(\Lambda^e_1 - \Lambda^h_1)^2 + \beta\Lambda^{e2}_4 - \gamma\Lambda^e_4(\Lambda^e_2 + \Lambda^h_1) ,$$

$$G^y_{bh} = \alpha\frac{1}{16}(3\Lambda^e_1 + \Lambda^e_2 + 4\Lambda^h_1)^2 + \beta\frac{1}{4}\Lambda^{e2}_4 + \gamma\frac{1}{8}\Lambda^e_4(3\Lambda^e_1 + \Lambda^e_2 + 4\Lambda^h_1) .$$

The parameters α, β and γ are defined by

$$\alpha = [1 + (C_{11} - C_{44})/\{(C_{11} - C_{44})^2 + 4C^2_{14}\}^{1/2}]/2 ,$$

$$\beta = [1 - (C_{11} - C_{44})/\{(C_{11} - C_{44})^2 + 4C^2_{14}\}^{1/2}]/2 ,$$

$$\gamma = 2C_{14}/\{C_{11} - C_{44})^2 + 4C^2_{14}\}^{1/2} ,$$

where C_{ij} are the components of the elastic modulus tensor.

(*) See V. I. Pustovoit and L. A. Poluektov : Zh. eksper. teor. Fiz. **50** (1966) 1265.